



1 **High-resolution simulation of link-level vehicle emissions and** 2 **concentrations for air pollutants in a traffic-populated East Asian city**

3
4 Shaojun Zhang ^{1,2}, Ye Wu ^{1,3*}, Ruikun Huang ¹, Han Yan ¹, Yali Zheng ^{1,4}, Jiming Hao ^{1,3}

5
6 ¹ School of Environment and State Key Joint Laboratory of Environment Simulation and Pollution
7 Control, Tsinghua University, Beijing 100084, China, Tsinghua University, Beijing 100084, P. R. China

8 ² Department of Mechanical Engineering, University of Michigan, Ann Arbor, MI 48109, U.S.

9 ³ State Environmental Protection Key Laboratory of Sources and Control of Air Pollution Complex,
10 Beijing 100084, P. R. China

11 ⁴ Society of Automotive Engineers of China, 102 Lianhuachi East Road, Beijing 100055, P.R. China

12 *Correspondence to:* Y. Wu (ywu@tsinghua.edu.cn)

13 14 **Abstract:**

15 Vehicle emissions of air pollutants created substantial environmental impacts on air quality for many
16 traffic-populated cities in East Asia. A high-resolution emission inventory is an irreplaceable tool
17 compared with traditional tools (e.g., registration data based approach) to accurately evaluate real-world
18 traffic dynamics and their environmental burden. In this study, Macao, one of the most populated cities
19 in the world, is selected to demonstrate a high-resolution simulation of vehicular emissions and their
20 contribution to air pollutant concentrations by coupling multi-models. First, traffic volumes by vehicle
21 category on 47 typical roads were investigated during weekdays of 2010 and further applied in a
22 networking demand simulation with the TransCAD model to establish hourly profiles of link-level
23 vehicle counts. Local vehicle driving speed and vehicle age distribution data were also collected in
24 Macao. Second, based on a localized vehicle emission model (e.g., the EMBEV-Macao), this study
25 established a link-based vehicle emission inventory in Macao with high resolution meshed in a temporal
26 and spatial framework. Furthermore, we employed the AERMOD model to map concentrations of CO,
27 NO₂ and primary PM_{2.5} contributed by local vehicle emissions during the weekdays of November 2010.
28 This study has discerned the strong impact of traffic flow dynamics on the temporal and spatial patterns
29 of vehicle emissions, such as a geographic discrepancy of spatial allocation up to 25% between THC
30 and PM_{2.5} emissions owing to spatially heterogeneous vehicle-use intensity between motorcycles and
31 diesel fleets. We also identified that local vehicles are a dominant source of ambient NO₂ in



1 traffic-populated areas as evidenced by good agreement between AERMOD-simulated data and
2 observed results. Therefore, this paper provides a case study and a solid framework for developing
3 high-resolution environment assessment tools for other vehicle-populated cities in East Asia.

4

5 **1. Introduction**

6 The soaring vehicle stock driven by social-economic development has created a series of
7 substantial challenges regarding air pollution, energy insecurity, and public health within many countries
8 (Uherek et al., 2010; Saikawa et al., 2011; Shindell et al., 2011; Walsh, 2014). At the national level, we
9 take nitrogen oxides (NO_x) emissions as an example as it is an essential precursor to the formation of
10 ozone and nitrate aerosol in the atmosphere. On-road vehicles are currently responsible for 29% of
11 national anthropogenic NO_x emissions in China (MEP, 2014), 37% in U.S. (U.S. EPA, 2014) and 40%
12 in Europe Union (EEA, 2014; Vestreng et al., 2009). At the city level, the vehicular contribution to
13 ambient nitrogen dioxide (NO₂) concentration is very significant in traffic related areas (Carslaw et al.,
14 2011). For example, in European countries where diesel vehicles make up a considerable part of private
15 passenger cars, near-road NO₂ concentration exceeds the ambient air quality standard. This issue is seen
16 as one of the most significant air pollution problems in Europe although great efforts have been made to
17 cope with the NO₂ exceedance, including the implementation of stringent emission standards for diesel
18 vehicles (e.g., the latest Euro 6 requirements) (Franco et al., 2014; Carslaw et al., 2011; Carslaw and
19 Rhys-Tyler, 2013; Chen and Borcken-Kleefeld, 2014). Higher health risk as a result of exposure to
20 vehicular emissions (e.g., particle, NO_x) is understandable in traffic-populated cities, and is probably
21 associated with the large resident population, greater traffic congestion and unfavorable dispersion due
22 to dense buildings (Du et al., 2012; Ji et al., 2012). In 2012, the International Agency for Research on
23 Cancer Group 1 assessed the carcinogenicity of diesel emissions as “carcinogenic to humans” with
24 sufficient evidence for it to be characterized as a cause of lung cancer (Benbrahim-Tellaa et al., 2012).

25 The high-resolution vehicle emission inventory is an irreplaceable tool to accurately evaluate
26 impacts on air quality and public health, as it can well reflect the close connections between
27 environmental impacts and traffic flows. McDonald et al. (2014) analyzed the impacts of enhanced
28 spatial resolution from 10 km to 500 m on vehicular CO₂ emission inventory for Los Angeles, which
29 clearly demonstrated substantial improvements in the accuracy for areas containing traffic-dense
30 microenvironments (e.g., heavily trafficked highways). Consequently, link-based emission inventory is a
31 preferred tool owing to its substantial advantage in spatial resolution for local traffic and environmental



1 management. Over the past decade, high-resolution emission inventory initiatives have been carried out
2 in China's vehicle-populated cities. Taking Beijing, the capital city of China for example, Huo et al.
3 (2009) established a link-based emission inventory for light-duty gasoline vehicles (LDGVs) in the
4 urban area based on estimated emission factors with the IVE model. However, significant emissions of
5 NO_x and fine particulate matter (PM_{2.5}) may be attributed to heavy-duty diesel vehicles (HDDVs)
6 instead of LDGVs, including the gross emitters registered in other provinces (Wang et al., 2011 and
7 2012a), whose contributions are currently not evidenced in the registration-based inventories for China's
8 vehicle-populated cities (Wu et al., 2011; Zhang et al., 2014a; Zheng et al., 2014). Wang et al. (2009)
9 and Zhou et al. (2010) estimated vehicular emissions for the urban area of Beijing by using grid-based
10 data of average speed and aggregated vehicle kilometers travelled. However, their resolutions are not
11 sufficient to present hourly fluctuation of network traffic volume and quantify vehicular emissions at the
12 link level.

13 As traffic management actions become more important for vehicle emission control, such as the
14 license control policies effective in seven vehicle-populated cities of China (e.g., Shanghai, Beijing,
15 Guangzhou, Tianjin, etc.) and the Electronic Road Pricing (ERP) program adopted in Singapore (Goh,
16 2002). We therefore envision greater demand for high-resolution vehicle emission inventories by local
17 environmental protection administrations in the near future. A few technical barriers are expected to be
18 shortly overcome for improving the high-resolution vehicular emission inventory based on the
19 development experience of the London Atmospheric Emission Inventory (LAEI) (TfL, 2014). First,
20 high-resolution traffic data including traffic counts, vehicle speed and fleet composition should be
21 investigated or estimated at the link level with hourly fluctuations. Second, real-world emission factors
22 should be developed based on a sufficient measurement database to effectively address potential
23 uncertainties (e.g., gaps between regulatory cycle and off-cycle conditions) (Carslaw et al., 2011; Wu et
24 al., 2012; Zhang et al., 2014a). Third, technology allocations of the total fleet (e.g., traffic counts by fuel
25 type and vehicle age) should be derived based on real-world traffic data instead of registration data,
26 considering vehicular emissions are fairly sensitive to vehicle technology allocations (Vallamsundar and
27 Lin, 2012). Finally, the application of high-resolution emission inventory can be significantly enhanced
28 by extending the evaluation framework from vehicular emissions to pollutant concentration, which are
29 of overriding concerns to residents, pedestrians and policy-makers (Vallamsundar and Lin, 2012; Misra
30 et al., 2013).



1 In this study, we selected Macao as a case city to demonstrate high-resolution simulation for
2 vehicle emissions and primary concentrations of air pollutants in this traffic-populated city. Macao is
3 well-renowned for its tourism and gaming industry, which attracts numerous visitors and created huge
4 transportation demand. Owing to the absence of massive rail-based public transit system, which is now
5 under construction in Macao, local transportation completely depends on on-road vehicles. The
6 vehicle-population density (including motorcycles, MCs) in Macao is approaching 7800 veh km⁻² in
7 2014, significantly more dense as compared with other East Asian cities (e.g., 430 veh km⁻² of Shanghai,
8 340 veh km⁻² of Beijing and 700 veh km⁻² of Hong Kong) (DESC, 2014; HKS, 2014; NBSC, 2014).
9 Furthermore, Macao's total vehicle population has surpassed 240 thousand in 2014, more than double
10 the level in 2000 (DESC, 2014). Significant gridlock has been caused due to rapid motorization in the
11 Macao Peninsula during rush hours, when the average speed of arterial roads is frequently lower than 15
12 km h⁻¹ (TMB, 2010). On the other hand, local air quality data indicate several nonattainment sites for
13 annual ambient PM_{2.5} and NO₂ concentrations in the traffic-dense and residential areas of Macao (DESC,
14 2014). On-road vehicles have been identified as the major local contributor to air pollution, because
15 industrial emissions in Macao are quite minor compared with the on-road transportation sector. Thus,
16 there is an urgent need to attach importance to controlling vehicular emissions with the support of
17 high-resolution emission inventory technology in this traffic-populated city.

18

19 2. Methodology and data

20 2.1 General study framework and components

21 This study generally consists of three components: (1) characterizing hourly traffic profiles at the
22 link level, (2) establishing a high-resolution vehicle emission inventory, and (3) simulating the
23 concentrations of major air pollutants contributed by local vehicle emissions in Macao (see Fig. 1). The
24 core task of this study is to calculate emissions of air pollutants and carbon dioxide (CO₂) from local
25 vehicles meshed in the high resolution matrix of the "hour-link-vehicle technology group", which is
26 illustrated by Equation 1.

$$27 \quad E_{h,l,p,v} = \sum_{f,y} 10^{-3} \cdot EF_{f,p,v,y} \cdot L_l \cdot TV_{h,l,v} \cdot VF_{f,v,y} \quad (1)$$

28 where $E_{h,l,p,v}$ are the emissions of pollutant category p from vehicle classification v during hour h for
29 link l, kg h⁻¹; $EF_{f,p,v,y}$ is speed-dependent average emission factor of pollutant category p for vehicle
30 technology group defined by classification v, fuel type f and vehicle age y, g veh⁻¹ km⁻¹; L_l is the total



1 length of link l , km; $TV_{h,l,v}$ is total traffic volume of vehicle classification f during hour h , veh h^{-1} ; and
2 $VF_{f,v,y}$ is the volume fraction of vehicle technology group defined by fuel type f and vehicle age y . We
3 define eight vehicle classifications in this study that were recognized from road traffic video records as
4 follow: light-duty passenger vehicle (LDPV), MC, taxi, public bus (PB), medium-duty passenger vehicle
5 (MDPV), heavy-duty passenger vehicle (HDPV), light-duty truck (LDT) and heavy-duty truck (HDT).

6 Therefore, we further characterized total hourly emissions from the total vehicle fleet based on the
7 bottom-up method, namely from each link to the entire road net, as Equation 2 illustrates.

$$8 \quad E_{h,p} = \sum_{l,v} E_{h,l,p,v} \quad (2)$$

9 where $E_{h,p}$ are the total vehicle emissions of pollutant category p during hour h from the total vehicle
10 fleet in Macao, kg h^{-1} . In the following two sub-sections, we present detailed methods for developing
11 high-resolution traffic data and vehicle emission factors. Due to the time limitation on the traffic field
12 investigation, we only focus the case study for weekdays during 2010; weekends were not investigated
13 when traffic flows might be different.

14

15 2.2 Summary of geography and road network in Macao

16 Macao is one of the two Special Administrative Regions (SAR) in China lies on the western side
17 of the Pearl River Delta, with a total land area of only 30 km^2 , which is the most densely populated city
18 in the world (~ 20 thousand people km^2) (DSEC, 2014). The Macao SAR now consists of the Macao
19 Peninsula (MP) and the Taipa-Cotai-Coloane (TCC) islands (See Fig. S1). In particular, the CoTai
20 Reclamation Area is a piece of newly reclaimed land on the top of the bay area between Taipa and
21 Coloane, where new casinos and hotels have been constructed since land of Macao is scarce. Nearly 90%
22 of Macao's total population is concentrated in the MP, where the population density is significantly
23 higher than the combined density of Taipa-CoTai-Coloane (TCC) regions (i.e., 54 thousand vs. 4.3
24 thousand, unit in people km^{-2}). The MP geographically consists of five regions, nominally parishes.
25 Among those five parishes, the St. Anthony Parish where the Ruins of St. Pual's Cathedral is located has
26 the highest population density, which is approaching 120 thousand people km^{-2} .

27 Based on the GIS database of road network in Macao provided by the Macao Transportation
28 Bureau, there were a total of 1704 road links in the study year of 2010. We categorized all those links
29 into three road classes: urban freeways, arterial roads and residential roads, representing that the level of
30 service decreasing from high to low. It should be noted that the road links are unevenly distributed



1 among various areas of Macao, but similar to the spatial patterns. For example, 77% of all road links
2 (i.e., 1306 links) were concentrated in the Macao Peninsula, which were responsible for 59% of Macao's
3 total road length.

4

5 **2.3 Field investigation and simulation of link-based traffic data**

6 We investigated traffic data on 47 typical road links during three field investigation periods from
7 Jan 2010 to Jan 2011 (i.e., nearly 20 weekdays during Jan 2010, May 2010 and Jan 2011), according to
8 the spatial heterogeneity of road network in Macao by covering all road classes and regions. The real
9 traffic flow records of each link was collected with a portable video camera for at least 20 minutes
10 within each hour. Among all links investigated, 5 typical road links were investigated for the entire day
11 (i.e., 24-h sampling). Sampling duration for the rest of the links investigated in general were from 6 a.m.
12 to 11 p.m. (i.e., day-time sampling). Detailed hourly traffic volumes by vehicle classification for 47 road
13 links were further broken down based on those original video profiles by major region and road class
14 (see Table 1). We can clearly observe variations in hourly total traffic counts for three road classes, with
15 significant peaks of traffic demand during morning and evening rush hours (see Fig. 2 and Table 1).

16 Traffic volume fraction by vehicle classification is another essential type of data obtained from
17 traffic video record (see Fig. S2 as an example of arterial roads). During the evening rush hour (6 p.m.),
18 LDPVs and MCs contributed nearly 80% of total traffic volume, which are the two major vehicle types
19 used for daily commuting demand in Macao. In particular, MCs are low-cost commuting vehicles for the
20 relatively lower income group in Macao. Therefore, the observed traffic fraction of MCs was higher
21 than that of LDPVs on arterial roads of the Macao Peninsula. By contrast, observed traffic fraction of
22 MCs in the TCC was only approximately 15%. In addition to the spatial variations among various road
23 classes and areas, we also observed temporal variations of various vehicle classifications. Taking arterial
24 roads in the MP for example, their average traffic fractions of taxis were approximately 10% during the
25 day time (6 a.m. to 12 p.m.). During the night time (12 p.m. to 6 a.m.), accompanied by significantly
26 reduced traffic demand of MCs and LDPVs, taxis could be responsible for 20~30% of total vehicle
27 counts. Due to the minor economic contribution of local industry, the average traffic fraction of trucks in
28 Macao indicating freight transportation was significantly lower than those in Beijing and Guangzhou.

29 The TransCAD 5.0 model was applied to estimate total traffic demand and its spatial allocation at
30 the link level. TransCAD 5.0, one of the most widely-used traffic planning software, can estimate
31 origin-destination (OD) matrix of the road network from link traffic counts. In this study, we selected



1 the multiple path matrix estimation (MPME) procedure provided by the TransCAD 5.0 and estimated
2 total traffic volumes of all road links during the 6 p.m. hour with observed hourly traffic counts of 33
3 links as input data. After a number of iteration runs, the average discrepancy between simulated traffic
4 volumes and the observed values (i.e., output vs. input) is 4.3% and the Pearson coefficient is 0.95,
5 indicating statistically satisfactory results (see Fig. S3). For other hours, we estimated hourly total traffic
6 volumes based on the averaged temporal allocations and simulated traffic volumes during the 6 p.m.
7 hour, as Equation 3 illustrates.

$$8 \quad TV_{h,l} = TV_{18,l} \cdot \frac{\overline{\alpha_{a,c,h}}}{\alpha_{a,c,18}} \quad (3)$$

9 where $TV_{h,l}$ is the hourly total traffic volume for road link l during the hour h , veh h^{-1} , and $TV_{18,l}$ is
10 particularly the hourly data during the 6 p.m. hour simulated by the TransCAD if observed traffic
11 volume data is unavailable); $\overline{\alpha_{a,c,h}}$ is the averaged ratio of hourly total traffic volume during the hour h
12 to daily total traffic volume for the area a and the road class c . Therefore, the traffic volumes by vehicle
13 classification are further estimated based on the traffic fraction data averaged by area, road class and
14 hour.

15 In addition to traffic volume, traffic condition indicated by link-based hourly speed is another
16 category of essential input data. First, we used a portable GPS receiver to collect second-by-second
17 vehicle trajectory data for on-road vehicles during the same field sampling periods of traffic counts.
18 Considering the distinctions of driving behaviors among MCs, PBs and other vehicle classifications (e.g.,
19 passenger vehicles and trucks), like more frequent stops for PBs to discharge and receive passengers, we
20 used a taxi equipped with the GPS receiver to chase LDPVs randomly to represent traffic conditions for
21 on-road vehicles other than PBs and MCs. Each targeted vehicle was chased for at least 10 minutes. For
22 PBs and MCs, we selected typical vehicles to record their traffic trajectory data. In this study, we
23 collected traffic trajectory data of LPDVs, PBs and MCs for 115 thousand seconds, 86 thousand seconds
24 and 30 thousand seconds, respectively, with high abundance of spatial and temporal distribution. Second,
25 we integrate the original second-by-second GPS trajectory data with the road network GIS system to
26 identify the road link information (e.g., link name, parish and road class) for each sampling second.
27 Third, we estimated averaged hourly speed for each road class in each parish. To validate the speed
28 profiles, we observed variations in average hourly speeds by area and road class for LDPVs as an
29 example, which were aggregated by link-level speed profiles with traffic volume data taken into account



1 (see Fig. 3). Clearly, average hourly speeds for arterial and residential roads in the MP were lower than
2 20 km h^{-1} for longer than 15 hours (e.g., from 6 a.m. to 8 p.m.), indicating extremely congested traffic
3 conditions. In particular, average hourly speeds during the evening rush period (e.g., 6 p.m. and 7 p.m.)
4 were even less than 15 km h^{-1} , which corresponded to the officially released data. In the TCC, where
5 traffic is less populated, average hourly speeds for arterial and residential roads were significantly higher
6 than those in the Macao Peninsula, ranging from 20 km h^{-1} to 40 km h^{-1} except for the 6 p.m. hour. On
7 the other hand, we could also observe differences of aggregated daily speed among various vehicle
8 classifications (see Fig. S4). For example, average daily speed of taxis was 24.0 km h^{-1} , higher than the
9 21.7 km h^{-1} of LDPVs, due to higher traffic volume fraction of taxis in the night time when there were
10 usually free traffic flows. Similarly, average speed of HDTs was 27.0 km h^{-1} , topping all vehicle
11 classifications, because their traffic volume fraction was significantly higher in the TCC compared to the
12 MP.

13

14 **2.4 Emission factor development and the integration with traffic data and vehicle age distribution**

15 We initiated a comprehensive measurement program of collecting real-world emission profiles
16 since 2010, in order to establish and update a localized emission factor model for vehicles in Macao (e.g.,
17 the EMBEV-Macao model). So far, more than 60 typical vehicles, LDPVs, taxis, PBs, LDTs and HDTs,
18 have been measured on road by using a portable emission measurement system (PEMS). Furthermore, a
19 large-scale remote sensing vehicle emission measurement project was conducted during March and
20 April 2008, which enabled the collection of fuel-based emission factors for MCs in Macao. Detailed
21 experimental section in Macao and the measurement results are documented in several of our previous
22 papers regarding gasoline, diesel and more advanced vehicles (e.g., hybrid electric vehicles) (Hu et al.,
23 2012; Wang et al., 2014; Zhang et al., 2014b; Zhou et al., 2014; Wu et al., 2015a and 2015b; Zheng et
24 al., 2015). We developed an emission factor model, the EMBEV-Macao model, with reference to the
25 modeling framework and methodology of the EMBEV model which is originally developed for the
26 vehicle fleet in Beijing (Zhang et al., 2014a). Technically, we used local measurement data to estimate
27 basic emission factors of air pollutants and CO_2 emissions under their typical driving conditions by
28 vehicle age group. Second, we developed localized speed correction curves based on a micro-trip
29 method for each vehicle classification to integrate vehicle emission factors and traffic conditions at the
30 link-level (Zhang et al., 2014b and 2014c; Wu et al., 2015). Furthermore, the EMBEV-Macao model
31 enables us to correct impacts of local temperature, fuel quality, air conditioning usage, and other aspects



1 to the real conditions. For example, the sulfur content of gasoline and diesel were approximately 90 ppm
2 and 15 ppm during 2010.

3 Considering that there was no significant policy influencing traffic flow composition during
4 2008-2010, we estimated detailed traffic fraction by fuel type and vehicle age for each vehicle
5 classification based on the vehicle information database from the 2008 remote sensing project (Zhou et
6 al., 2014). It should be noted that some vehicle classifications have a single fuel type; e.g., gasoline for
7 MCs and diesel for PBs. By contrast, other vehicle specifications like engine displacement have a more
8 important effect on real-world emissions. Therefore, we also derived the on-road traffic volume split
9 ratios by engine displacement for MCs and PBs (refer to the footnote of Table 2). Table 2 illustrates the
10 detailed traffic volume fraction by vehicle age and fuel type (or split by engine displacement for MCs
11 and PBs) for each vehicle classification.

12

13 **2.5 Modeling dispersion of vehicular air pollutants**

14 Urban air quality models are commonly used to estimate the spatial distribution of vehicular
15 pollutants by simulating their chemical and physical processes in the atmosphere within urban areas.
16 Holmes and Morawska (2006) classified dispersion models into Box models, Gaussian models,
17 Lagrangian models, Computational Fluid Dynamic (CFD) models. Currently, Gaussian models are
18 recommended by the environmental protection agency of most countries all over the world.

19 The AMS/EPA regulatory model (AERMOD) is a steady state Gaussian plume dispersion model
20 which is recommended by U.S. EPA (U.S. EPA, 2004). The modeling system consists of one main
21 program (AERMOD) and two pre-processors (i.e., AERMET and AERMAP). In addition, calculating
22 urban boundary layer parameters and considering urban heat island effect makes AERMOD sensitive for
23 local meteorological conditions. Recently, several studies have investigated the integration performances
24 of the traffic simulation model, vehicle emission model and the AERMOD model. For example,
25 Vallamsundar and Lin (2012) integrated MOVES and AERMOD models to simulate the PM_{2.5} hotspot
26 cases of typical roads in U.S. cities (i.e., study domain area of ~0.5 km²) and provided some
27 implications based on sensitivity analysis, such as narrowing the data gap between traffic, emissions and
28 air quality models and further investigation of important local input data (e.g., traffic composition, fleet
29 age distribution). Misra et al. (2013) also integrated a traffic simulation model, a vehicle emission model
30 and the AERMOD model to estimate traffic-related pollution in downtown Toronto (i.e., study domain
31 area of ~0.5 km²). It should be noted that, in those previous investigations at near-field level (Zannetti,



1 1990), the AERMOD simulated vehicular emissions as a series of point sources which approximate a
2 traffic lane.

3 Considering a significantly larger study area, higher road density and the scarcity of metrological
4 data and surrounding building profiles in a sufficiently fine resolution, we divided the study domain into
5 a grid of 350 square cells (500 m×500 m). Aggregated hourly vehicular emissions of major pollutants
6 (e.g., CO, NO_x and PM_{2.5}) from all road links in each grid are used as the input data for the AERMOD.
7 The receptors are placed at central points of all cells at a height of 2.0 m. In terms of the geographic data
8 and the altitude information is obtained from the Google Earth. Building downwash effects are
9 simulated by the AERMOD. In our study, we model the weekdays of November 2010 when rainy days
10 were much fewer compared to other months. Hourly meteorological profiles from two monitoring sites
11 located in MP and TCC respectively, including temperature, wind direction, wind speed, relative
12 humidity and air pressure are provided by the Department of Metrological Services in Macao. The
13 northeasterly winds are prevailing during that month, supplemented by a minor part of northerly and
14 easterly winds (see Fig. S5). Based on the fleet composition and on-road measurement data, we
15 estimated average volume ratio of primary NO₂ to total NO_x emissions as) 10%. In addition, ozone
16 concentration data from Macao EPB are also used to simulate the oxidation process from freshly emitted
17 NO to ambient NO₂ by the AERMOD.

18 In order to compare simulated concentrations of air traffic-related pollutants with their ambient
19 concentrations over the same period (i.e., November 2010), air quality data of local monitoring sites are
20 provided by the Macao Environmental Protection Bureau (EPB). Furthermore, impacts from regional
21 background, cross-boundary transport and other area sources are estimated by closing local stationary
22 (e.g., power and waste incineration plants located in the Coloane Island) and on-road sectors with the
23 CMAQ model at a spatial-resolution level of 4×4 km², which add up to 304 μg m⁻³ of CO, 27 μg m⁻³ of
24 NO₂ and 23 μg m⁻³ of PM_{2.5} as the monthly averages. Meanwhile, we employed the AERMOD and
25 estimated that NO₂ concentration contributed by local power and waste incineration plants located in
26 Coloane were approximately 1 μg m⁻³ in the Coloane Island and more marginal in the MP.

27

28 **3. Results and discussion**

29 **3.1 Estimated traffic activity and vehicle emissions**

30 Table 3 presents spatially-explicit traffic counts during a typical weekday and an evening rush
31 hour (i.e., 6 p.m.), respectively. More than 80% of total daily traffic counts were concentrated in the MP,



1 160% higher than the overall average of Macao. In particular, the Saint Antony Parish with
2 internationally-renowned tourist attraction (e.g., the Ruins of St. Paul's) had a top hour-based density of
3 daily traffic volume as a result of its substantial population density. Furthermore, traffic activity (unit
4 veh km h⁻¹ or veh km d⁻¹) can be estimated as the product of traffic counts and link length, namely
5 $TV_{h,l,v}$ and L_l (see Equation 1), which is an essential indicator of vehicle-use intensity. Estimated
6 daily traffic activity of Macao's total vehicles in a typical weekday of 2010 is 4.04×10^6 veh km d⁻¹ (see
7 Table S1). LDPVs and MCs rank first and second among all vehicle classifications, accounting for 43%
8 and 30% of total daily traffic activity in Macao. Therefore, fleet-average daily vehicle kilometers
9 travelled (VKT) of LDPVs and MCs during weekdays of 2010 are 20.8 km and 11.7 km, respectively. If
10 we ignore potential difference between weekdays and weekends, fleet-average annual VKT of LDPVs
11 and MCs registered in Macao are 7600 km and 4300 km as of 2010, which are quite comparable with
12 our previous survey results. Those values could be only responsible for traffic demand within Macao,
13 considering a part of LDPVs travel cross the boundary of the Macao SAR into Mainland China. It is
14 worth noting that annual VKT of LDPVs registered in Macao is significantly lower than those of Beijing
15 and Guangzhou (Zhang et al., 2013 and 2014a). The major reason is the scale of Macao is much smaller
16 than those megacities of Mainland China (e.g., Beijing, Guangzhou), approximately 15 km from the
17 northernmost parish in MP to the Coloane Island. Since fewer MCs drive on the cross-sea bridges, a
18 major part of MCs' traffic activity (note: in particular for light-duty two-stroke MCs) is largely limited
19 within MP or TCC. Therefore, traffic activity of MCs is lower than LDPVs although with higher traffic
20 counts, whose estimated annual VKT is comparable to the value in Mainland China (e.g., 5000~6000
21 km) (Zhang et al., 2013 and 2014a).

22 Table 4 presents estimated average distance-specific emission factors of major air pollutants by
23 vehicle classification and fuel type for that typical weekday in Macao during 2010. Average CO and
24 THC emission factors for gasoline powered LDPVs in Macao are significantly lower by 57% and 30%,
25 respectively, compared to those of gasoline LDPVs registered in Beijing, although the average driving
26 speed of LDPVs in Macao is lower than Beijing (e.g., ~22 km h⁻¹ vs. 30 km h⁻¹). A major reason for that
27 estimation is a majority of the gasoline cars are imported from Japan, where vehicle emission standards
28 are in general more stringent than those implemented in Mainland China (Wang et al., 2014). By
29 contrast, compared to gasoline taxis in Beijing, diesel engines applied in the taxi fleet in Macao led to
30 significantly higher NO_x and PM_{2.5} emission factors by 3.5 times and 17 times (Hu et al., 2012; Zhang
31 et al., 2014a). For heavy-duty trucks and buses, lower speed and a higher proportion of older vehicles



1 result in higher NO_x and $\text{PM}_{2.5}$ emission factors for those heavy-duty diesel vehicles in Macao than
2 those in Beijing. For MCs, in particular light-duty two-stroke MCs, their fleet-average THC emission
3 factors are significantly higher than other vehicle technology types (Zhou et al., 2014).

4 Estimated total vehicular emissions in a typical weekday during 2010 are 17.5 tons of CO, 3.60
5 tons of THC, 5.04 tons of NO_x and 0.28 tons of $\text{PM}_{2.5}$. As Fig. 4 illustrates, emission allocation patterns
6 by vehicle classification are different for various pollutant categories. Compared to well-controlled CO
7 and THC emission factors of LDPVs, MCs are estimated to have been responsible for 66% and 72% of
8 total vehicular emissions for CO and THC respectively. In particular, two-stroke MCs contribute 45% of
9 total THC vehicular emissions, which led Macao government to initiate a replacement of two-stroke
10 MCs with small-size four-stroke MCs after 2010. Further, a possible promotion of electric MCs in
11 Macao is also under consideration by policy-makers in Macao. For both NO_x and $\text{PM}_{2.5}$, diesel-powered
12 passenger fleets contributed 60~65% of total vehicular emissions, including PBs, taxis and HDPVs
13 mainly owned by hotels and casinos. By contrast, diesel trucks contributed approximately ~10% of total
14 NO_x and $\text{PM}_{2.5}$ emissions in Macao, substantially lower than the contribution of diesel trucks registered
15 in other populated cities of China (e.g., 30~35% for Beijing and Guangzhou) (Zhang et al., 2013 and
16 2014a). This phenomenon should be attributed to the significantly higher passenger transportation
17 demand than freight transportation in Macao, as tourism and entertainment industry is the pillar of the
18 local economy. Our results clearly suggest policy-makers in Macao should carefully focus on various
19 vehicle classifications when facing emission mitigation targets for various air pollutants.

20 For CO_2 emissions, unfavorable operating conditions like lower driving speeds and frequent use of
21 air-conditioning systems resulted in substantial climate and energy penalties for passenger vehicles (e.g.,
22 LDPVs, taxis, PBs). For example, the estimated average CO_2 emission factor of LDPVs is 263 g km^{-1}
23 (see Table 4), a significant increase of approximately 25% compared to on-road measurement results
24 under a higher average speed ($205\sim 210 \text{ g km}^{-1}$ at 30 km h^{-1}). This is equivalent to ~13 L per 100 km
25 fuel consumption, indicating a substantial increase of CO_2 and fuel consumption under real-world
26 driving conditions than those measured under the type-approval conditions applied in current regulatory
27 systems (e.g., both Japan and Europe). Overall, the estimated total CO_2 emissions from all vehicle
28 classifications and all road links are 1001 tons during a typical day. LDPVs, PBs and taxis are estimated
29 to have been responsible for 46%, 14% and 12% of total daily CO_2 emissions, respectively (see Fig. 4),
30 ranking in the top three among all classifications.



1 Our previous evaluation indicates estimated macro uncertainty (i.e., annual emission inventory by
2 using registration data) for air pollutants (e.g., CO, THC, NO_x and PM_{2.5}) is approximately -30%/+50%
3 at a 95% confidence level (Zhang et al., 2014a). The skewed probability distribution is due to high
4 emitters of air pollutants within the fleet. The uncertainty in CO₂ emissions would be narrower due to
5 detailed localized vehicle information and fuel economy data are used in estimation, plus it is strongly
6 corrected by average speed. However, if the evaluation level is refined into a link-level, the uncertainty
7 in vehicle emissions would be greater due to traffic flows became inherently greater as the spatial
8 resolution was enhanced. We could address the uncertainty in link-level vehicle emissions with the
9 traffic big data (see the discussion in the next sub-section) available for typical roads in the future.

10

11 **3.2 Temporal and spatial variations in traffic-related emissions**

12 High strong correlations between temporal variations in traffic activity and emissions are clearly
13 observed for all air pollutants and CO₂ ($R^2 > 0.92$, see Fig. 5). For example, the 6 p.m. hour contributed
14 6.9% of total daily traffic activity, when hourly emissions of gaseous species (CO, THC, NO_x and CO₂)
15 were responsible for 7.9%~8.7% of their daily emissions. This was because emission factors of gaseous
16 pollutants and CO₂ were increased during the rush hours due to lower driving speed. The increases were
17 15%~26% for their emission factors compared to the daily averages. Compared with the night time,
18 average gaseous emission factors of the total fleet were increased by 54%~120%. The elevation of PM_{2.5}
19 emissions in the rush hour was not as significant as gaseous species, because the traffic demand of diesel
20 fleets (e.g., HDPVs, taxis, PBs, trucks) was increased less relative to gasoline fleets (e.g., MCs, LDPVs)
21 in Macao.

22 Spatial distributions of vehicular emissions are associated with real-world traffic characteristics
23 including total traffic counts, traffic conditions and fleet composition. To sum up, 58% of NO_x, 52% of
24 PM_{2.5} and 59% of CO₂ vehicular emissions were estimated from the road network of the MP (see Fig. 6
25 for NO_x, Fig. S6 for other pollutants and Table S2 for the summary of spatial distribution). Meanwhile,
26 74% of CO and 77% of THC emissions were aggregated from on-road vehicles within the MP. The
27 discrepancy of emission spatial allocations between CO/THC and NO_x/PM_{2.5}/CO₂ is primarily because
28 the higher fleet penetration of MCs in the MP. That is to say, relative inaccuracy associated with
29 emission spatial allocation by the top-down approach could be up to 20% if real-world fleet composition
30 information is not taken into account. By contrast, the spatial allocations of NO_x, PM_{2.5} and CO₂ at three
31 cross-sea bridges were estimated to be higher by approximately 50~110% than CO and THC, because



1 the traffic volume fraction of MCs was significantly lower than in other regions, in particular compared
2 with the MP.

3 Detailed statistical profiles of spatial-related vehicular emission are summarized by length-specific
4 emission intensity of road groups and area-specific emission intensity of gridded cells (see Table 5 and
5 Table 6). Higher length-specific emission intensities of CO and THC are unexpectedly identified on
6 arterial roads in the MP with less traffic accounts compared with their urban freeway counterparts,
7 owing to higher traffic activity of MCs and more severe traffic congestion increasing all-fleet emission
8 factors. For NO_x, PM_{2.5} and CO₂, higher length-specific emission intensities are all associated with
9 higher level of service for the three road classes, both in the MP and the TCC. Area-specific emission
10 intensities of all pollutants and CO₂ had decreasing trends from north to south (i.e., from the MP to the
11 Coloane Island), similar to the patterns of road density and traffic demand. Emission hotspots are
12 identified in traffic-populated cells of the MP, e.g., the region close the Ruins of St. Paul's, where daily
13 area-specific emission intensity was as high as 600 kg km⁻² d⁻¹. This level is ~4 times of that in the entire
14 Macao and ~40 times of the Coloane Island. Not surprisingly, significant near-field air pollution
15 problems in MP are caused by those extremely higher vehicular emissions which will be in addressed in
16 detail in the following sub-section.

17 It should be noted that increasingly board application of an intelligent traffic system (ITS) and
18 smart vehicle technologies can play a significant role in improving our understanding of dynamic traffic
19 flows, namely enabling the big data collection regarding total traffic volume, fleet composition and
20 traffic conditions (e.g., speed). For example, the traffic loop detector (TLD) and the vehicle license plate
21 recognition (VLPR) are both widely-used and economic ITS technologies that began in the early 2000s
22 in China and are integrated to provide category-informed vehicle volume, on which many cities in China
23 (e.g., Beijing, Guangzhou) depend to release official data including year-by-year variations in total
24 urban traffic demand (BJTRC, 2013; Zhang et al., 2013). The traffic loop detector is able to provide
25 vehicle passing speed, however, which is often criticized due to the poor representative for the entire
26 trips or entire traffic network. The floating car system, namely using the taxi fleet as probe vehicles
27 based on GPS technology, is an advanced monitoring tool for real-time traffic conditions. Taking
28 Beijing for example, its floating car system is capable of mapping link-based traffic conditions for the
29 urban area (~1000 km²) every five minutes based on 66 thousand taxis and mesh urban average speed
30 layer down at a link level. During 2012, 24-h average speeds of the urban area of Beijing were estimated
31 at 23.2±2.3 km h⁻¹ for weekdays and 26.9±3.9 km h⁻¹ for weekends and holidays, respectively



1 (BJTRC, 2014; Zhang et al., 2014a and 2014b). Therefore, daily variations in traffic conditions could
2 result in a coefficient of variation (i.e., the ratio of standard deviation to mean value) of 6% for the
3 distance-specific CO₂ emission factor all year around. Most recently, the radio frequently identification
4 (RFID) technology has been applied in a few Chinese cities (e.g., Nanjing, the capital city of Jiangsu
5 province) to provide more accurate vehicle recognition with detailed specifications (e.g., category, fuel
6 type, emission standard, model year, and vehicle size) than the TLD and the VLPR. The RFID data in
7 Nanjing are further connected with a smartphone application, based on which more capabilities like
8 environmentally-constrained traffic management (e.g., low emission zone, congestion fee program)
9 could be developed in the future. From the perspective of vehicles, for instance, more real vehicle data
10 can be accessed through the on-board diagnostic (OBD) decoders. The second-by-second data of driving
11 conditions (e.g., speed, acceleration) are able to be combined with operating mode-based (e.g.,
12 VSP-informed) emission model to provide finer emission estimations. While foregoing advanced traffic
13 data collection methods are not available in Macao, the framework of this study is technically feasible to
14 large cities in China when the traffic big data are adequately available.

15

16 **3.3 Simulated concentrations of primary traffic-related pollutants in Macao**

17 Fig. 7 presents a spatial map of average concentrations of primary vehicle-contributed NO₂ (see
18 CO and PM_{2.5} in Fig. S7), which shows the simulated results of all receptors (i.e., central points of cells)
19 with the AERMOD model. The spatial variations in simulated concentrations highly resemble the
20 patterns of area-specific emission intensity for vehicular pollutants. For example, average concentrations
21 contributed by local vehicular emissions in Macao were $87.7 \pm 89.4 \mu\text{g m}^{-3}$ of CO, $22.2 \pm 17.1 \mu\text{g m}^{-3}$ of
22 NO₂ and $1.30 \pm 0.91 \mu\text{g m}^{-3}$ of PM_{2.5}, respectively (see Table 6). Highest receptor concentrations of CO,
23 NO_x and PM_{2.5} are 424, 84.9 and $4.42 \mu\text{g m}^{-3}$, respectively, all occurring at traffic-populated cells in the
24 MP.

25 We further compared modeled concentrations of primary pollutants from local vehicles and
26 official air quality data. Traffic contributions at the monitoring sites are approximated by simulated
27 results for their closest receptors as to estimate monthly-average source proportions of on-road vehicles
28 in Macao. Therefore, source proportions vary from pollutant categories and locations during the time
29 framework of this study. For example, estimated proportions of vehicular CO emissions are ~25-30% in
30 the MP and ~15% in the Taipa Island, indicating lower impacts compared to regional contributions. For
31 NO₂, significantly high local contributions are identified. For example, for two monitoring sites in



1 residential areas, 50-55% of monitored NO₂ concentrations are caused by local vehicles. The proportion
2 for the site located in traffic-populated area is estimated over 80%. The contribution proportion of
3 on-road vehicles is estimated predominantly in the traffic-dense area. With regard to PM_{2.5}, estimated
4 proportions of primary vehicular PM_{2.5} emissions are approximately 3% in residential areas and 5% in
5 traffic-populated area. It should be acknowledged that the atmospheric secondary PM_{2.5} considerably
6 contributed by vehicle emissions is not considered in this study, which need to be applied with a very
7 detailed regional emission inventory including all anthropogenic emission sources and complex air
8 quality models with sophisticated source apportionment functions. This is beyond the scope of this
9 paper.

10 Hence, we compared daily NO₂ concentrations during 19 weekdays of November 2010 between
11 simulated results and observed concentrations for one monitoring site in the MP (see Fig. 8), because
12 another air monitoring site in the MP is very close to the city boundary (i.e., less than 300m) and greatly
13 influenced by vehicle emissions in Zhuhai (i.e., the adjacent city to Macao). We observe a reasonable
14 correlation (Pearson's R=0.67) between simulated results and observed concentration for this site. The
15 average discrepancy between simulated and observed concentrations is $15 \pm 22\%$, which may probably
16 be attributed to the following aspects but not limited to: (1) uncertainty in estimating background level
17 and regional transport by using CMAQ since Macao only covers two CMAQ cells; (2) the
18 approximation of the receptor of AERMOD and the air quality monitoring sites; (3) the strong
19 street-canyon effects in the building-dense MP which are not sophisticatedly addressed by the
20 AERMOD. For example, Sheng and Tang (2011) coupled the OSPM model and detailed building-based
21 geography layer and derived hotspots of traffic-related NO₂ concentrations that were simulated higher
22 than 62 ppb (i.e., $127 \mu\text{g m}^{-3}$) in 2004. Although their emission factors estimated with the MOBILE
23 model (Tang et al., 2006) were lower than ours based on local PEMS measurement, their higher results
24 could be attributed to the significant street canyon effect and higher spatial resolution (i.e., 319 receptors
25 km^{-2}) compared with our study. Furthermore, specifically for hotspots, advanced computational fluid
26 dynamics (CFD)-based micro-scale air quality model coupled with sophisticated gaseous chemical
27 mechanisms and aerosol dynamics are suggested to quantitatively assess potential impacts and
28 mitigation strategies from perspectives of traffic flows, weather conditions and architecture layout.
29 Given the severe traffic congestion in Macao, which is an unfavorable condition for some advanced
30 deNO_x after-treatment devices (e.g., selective catalyst reduction for diesel commercial vehicles), other
31 effective mitigation alternatives should be carefully considered by local policy-makers such as a



1 substantial penetration of alternative fuel and advanced powertrain systems to the public fleets in Macao
2 (e.g., dedicated natural gas buses, hybrid electric taxis and battery electric taxis/buses) (Zhang et al.,
3 2014d; Wang et al., 2015; Wu et al., 2015).

4

5 **4. Conclusions**

6 High-resolution vehicle emission inventory is an irreplaceable assessment tool to achieve the fine
7 air quality administration, in particular for traffic-populated East Asian cities where traffic management
8 is an essential approach to reduce emissions. Due to the difficulties in obtaining link-level traffic flow
9 data and localized emission measurement profiles, such a dedicated environmental tool has not been
10 developed at the link-level which covers a whole city and all vehicle categories. This study selected the
11 entire area of Macao, the most populated city in this world, to demonstrate a high-resolution simulation
12 of vehicular pollution by coupling detailed local data collected and inter-disciplinary models (e.g., traffic
13 demand).

14 Our traffic flow investigation and simulation results showed that total daily traffic activity during a
15 typical weekday of 2010 was estimated at 4.06 million veh km d⁻¹. Passenger trips using MCs, LDPVs,
16 taxis and buses were responsible for a dominant part of travel demand in Macao, accompanied by a
17 significantly less traffic fraction of on-road freight transportation (e.g., trucks) than other cities in
18 Mainland China. Spatial heterogeneity of traffic flow characteristics has been discerned between the MP
19 and the remaining parts (i.e., the TCC) of Macao. For example, the MP contributed over 80% of total
20 traffic accounts in Macao during a weekday of 2010 and MCs were more prevalent in this more
21 populated peninsula compared to the TCC. Tremendous travel demand created during rush hours
22 resulted in significant traffic congestion, indicated by an average speed lower than 15 km h⁻¹ for arterial
23 and residential roads in the MP.

24 Based on a localized vehicle emission model (e.g., the EMBEV-Macao) and high-resolution traffic
25 profiles regarding traffic volume, average speed and fleet composition, this study established a
26 link-based vehicle emission inventory with high resolution meshed in a temporal and spatial framework
27 (e.g., hourly and link-level). We estimated that total daily vehicle emissions in Macao were 17.5 tons of
28 CO, 3.60 tons of THC, 5.04 tons of NO_x and 0.28 tons of PM_{2.5} during a typical weekday of 2010. MCs
29 are the major contributor to CO and THC emissions due to their higher emission factors than LDPVs.
30 Diesel-powered passenger fleets like buses and taxis contributed 60~65% of total vehicular emissions of
31 NO_x and PM_{2.5}. With a special focus on the MP region, where traffic density and congestion are more



1 significant, area-specific emission intensity can be higher than the average of the entire Macao area by
2 135% for CO, 145% for THC, 85% for NO_x, 65% for PM_{2.5} and 90% for CO₂. The geographic
3 discrepancy of spatial allocation between THC and PM_{2.5} emissions can be attributed to the spatially
4 heterogeneous vehicle-use intensity between MCs and diesel fleets (e.g., higher use intensity of MCs in
5 the MP); and this trait could not be identified by using the traditional emission inventory tool. From the
6 perspective of temporal variations, hourly emissions of CO, THC, NO_x and CO₂ during the evening
7 traffic peak could be responsible for 7.9%~8.7% of total daily emissions, when their emission factors
8 were increased by 15%~26% compared to the daily averages due to the traffic congestion.

9 We further employed the AERMOD model to quantify average concentrations of CO, NO₂ and
10 PM_{2.5} contributed by primary vehicle emissions in Macao. Our simulation indicated receptor-averaged
11 concentrations from primary vehicle emissions were $87.7 \pm 89.4 \mu\text{g m}^{-3}$ of CO, $22.2 \pm 17.1 \mu\text{g m}^{-3}$ of
12 NO₂ and $1.30 \pm 0.91 \mu\text{g m}^{-3}$ of PM_{2.5}, respectively, during the weekdays of November, 2010. The
13 highest receptor concentrations of CO, NO_x and PM_{2.5} were $424 \mu\text{g m}^{-3}$, $84.9 \mu\text{g m}^{-3}$ and $4.42 \mu\text{g m}^{-3}$,
14 respectively, all occurring at traffic-populated cells in the MP. On-road vehicles are a dominant source
15 of ambient NO₂ in traffic-populated areas as indicated by the good agreement between
16 AERMOD-simulated data and observed results. This paper can provide a useful case study and a solid
17 framework for developing high-resolution environmental assessment tools for other vehicle-populated
18 cities in the world. We also highlighted the importance of real traffic data using ITS techniques and the
19 traffic big data approaches to future high-resolution simulation for larger cities in the East Asia and all
20 over the world.

21
22 *Acknowledgments.* This work was sponsored by the National High Technology Research and
23 Development Program (863) of China (No. 2013AA065303), the National Natural Science Foundation
24 of China (No. 51322804 and No. 51378285), and the Program for New Century Excellent Talents in
25 University (NCET-13-0332). We thank Mr. Jiandong Wang and Miss Xiao Fu of Tsinghua University
26 for their great help in running the CMAQ Model. The contents of this paper are solely the responsibility
27 of the authors and do not necessarily represent official views of the sponsors.

28



1 References

- 2 Benbrahim-Tallaa, L., Baan, R.A., Grosse, Y., Lauby-Secretan, B., Ghissassi, F.E., Bouvard, V., Guha, N.,
3 Loomis, D., Straif, K.: Carcinogenicity of diesel-engine and gasoline-engine exhausts and some
4 nitroarenes. *Lancet Oncol.*, 13(7), 663-664, 2012
- 5 Beijing Transport Research Center: Beijing Transportation Annual Report 2013. 2014 (accessed), available at:
6 www.bjtrc.org.cn
- 7 Carslaw, D.C., Beevers, S.D., Tate, J.E., Westmoreland, E.J., Williams, M.L.: Recent evidence concerning higher
8 NO_x emissions from passenger cars and light duty vehicles. *Atmos. Environ.*, 45(39), 7053-7063, 2011.
- 9 Carslaw, D.C., Rhys-Tyler, G.: New insights from comprehensive on-road measurements of NO_x, NO₂ and NH₃
10 from vehicle emission remote sensing in London, UK. *Atmos. Environ.*, 81, 339-347, 2013.
- 11 Chen, Y., Borken-Kleeefeld, J.: Real-driving emissions from cars and light commercial vehicles – Results from 13
12 years remote sensing at Zurich/CH. *Atmos. Environ.*, 88, 157-164, 2014.
- 13 Department of Statistics and Census Service (DSEC), Macao: Statistical Information System of Macao. 2014
14 (accessed). Available at <http://www.dsec.gov.mo/default.aspx>
- 15 Du, X., Wu, Y., Fu, L., Wang, S., Zhang, S., Hao, J.: Intake fraction of PM_{2.5} and NO_x from vehicle emissions in
16 Beijing based on personal exposure data. *Atmos. Environ.*, 57, 233-243, 2012.
- 17 EEA (European Environmental Agency): European Union emission inventory report 1990–2012 under the
18 UNECE Convention on Long-range Transboundary Air Pollution (LRTAP). Annex I_European Union
19 (EU-27) LRTAP emission data. 2014. Available at <http://www.eea.europa.eu/publications/lrtap-2014>
- 20 Franco, V., Sánchez, F.P., German, J., Mock, P.: Real-world exhaust emissions from modern diesel cars. The
21 International Council on Clean Transportation Report, 2014. Available at
22 <http://www.theicct.org/real-world-exhaust-emissions-modern-diesel-cars>
- 23 Goh, M.: Congestion management and electronic road pricing in Singapore. *J. Transp. Geogr.*, 10(1), 29-38, 2002.
- 24 HKCSD (Hong Kong Census and Statistics Department): Hong Kong Statistics, 2014. Available at
25 <http://www.censtatd.gov.hk/hkstat/index.jsp>
- 26 Holmes, N.S., Morawska, L.: A review of dispersion modelling and its application to the dispersion of particles:
27 An overview of different dispersion models available. *Atmos. Environ.*, 40(30), 5902-5928, 2006
- 28 Hu, J., Wu, Y., Wang, Z., Li, Z., Zhou, Y., Wang, H., Bao, X., Hao, J.: Real-world fuel efficiency and exhaust
29 emissions of light-duty diesel vehicles and their correlation with road conditions. *J. Environ. Sci.*, 24(5),
30 865-874, 2012.
- 31 Huo, H., Zhang, Q., He, K., Wang, Q., Yao, Z., Streets, D.: High-resolution vehicular emission inventory using a
32 link-based method: a case study of light-duty vehicles in Beijing. *Environ. Sci. Technol.*, 43(7),
33 2394-2399.
- 34 Ji, S., Cherry, C.R., Bechle, M.J., Wu, Y., Marshall, J.D.: Electric vehicles in China: emissions and health impacts.
35 *Environ. Sci. Technol.*, 46(4), 2018-2024, 2012.
- 36 MEP (Ministry of Environmental Protection, P. R. China): Bulletin of China's Environmental Status in 2013.
37 2014. Available at <http://jcs.mep.gov.cn/hjzl/zkgb/2013zkgb> (in Chinese)
- 38 Misra, A., Roorda, M.J., MacLean, H.L.: An integrated modelling approach to estimate urban traffic emissions.
39 *Atmos. Environ.*, 73, 81-91: 2013
- 40 McDonald, B.C., McBride, Z.C., Martin, E.W., Harley, R.A.: High-resolution mapping of motor
41 NBSC (National Bureau of Statistics of China): China Statistical Yearbook, 2014.



- 1 Saikawa, E., Kurokawa, J., Takigawa, M., Borken-Kleefeld, J., Mauzerall, D.L., Horowitz, L.W., Ohara, T.: The
2 impact of China's vehicle emissions on regional air quality in 2000 and 2020: a scenario analysis. *Atmos.*
3 *Chem. Phys.*, 11, 9465-9484, 2011.
- 4 Shindell, D., Faluvegi, G., Walsh, M., Anenberg, S.C., van Dingenen, R., Muller, N.Z., Austin, J., Koch, D.,
5 Milly, G.: Climate, health, agricultural and economic impacts of tight vehicle-emission standards. *Nature*
6 *Climate Change*, 1, 59-66, 2011.
- 7 Sheng, N., Tang, U.W.: A building-based data capture and data mining technique for air quality assessment. *Front.*
8 *Environ. Sci. Engin. China*, 5(4), 543-551, 2011.
- 9 Tang, U.W., Wang, Z.: Determining gaseous factors and driver's particle exposure during traffic congestion by
10 vehicle-following measurement techniques. *J. Air Waste Manag. Assoc.*, 56(11), 1532-1539, 2006
- 11 Transportation Bureau of Macao (TBM: Consultation report on the road transportation policy planning of Macao
12 2010-2020. 2010. Available at <http://www.dsat.gov.mo/ptt/sc/doc.pdf>
- 13 Transport for London: London Atmospheric Emissions Inventory 2010, Methodology Document. 2014 (assessed),
14 available at <http://data.london.gov.uk/dataset/london-atmospheric-emissions-inventory-2010>
- 15 Uherek, E., Halenka, T., Borken-kleefeld, J., Balkanski, Y., Bernsten, T., Borrego, C., Gauss, M., Hoor, P.,
16 Juda-Rezler, K., Lelieveld, J., Melas, D., Rypdal, K., Schmid, S.: Transport impacts on atmosphere and
17 climate: Land transport. *Atmos. Environ.*, 44(37), 4772-4816, 2010.
- 18 U.S. EPA (U.S. Environmental Protection Agency): AERMOD: Description of model formulation, 2004.
19 Available at http://www.epa.gov/scram001/7thconf/aermod/aermod_mfd.pdf
- 20 U.S. EPA: The 2011 National Emissions Inventory (NEI), 2014 (accessed). Available at
21 <http://www.epa.gov/ttn/chief/net/2011inventory.html>
- 22 Velders, G. J. M., Geilenkirchen, G. P., Lange, R. d.: Higher than expected NO_x emission from trucks may affect
23 attainability of NO₂ limit values in the Netherlands. *Atmos. Environ.*, 45, 3025-3033, 2011.
- 24 Vestreng, V., Ntziachristos, L., Semb, A., Reis, S., Isaksen, I.S.A., Tarrasón, L.: Evolution of NO_x emissions in
25 Europe with focus on road transport control measures. *Atmos. Chem. Phys.*, 9, 1503-1530, 2009.
- 26 Vallamsundar, S., Lin, J.: MOVES and AERMOD used for PM_{2.5} conformity hot spot air quality modeling. *J.*
27 *Trans. Res. Board*, 2270, 39-48, 2012.
- 28 Walsh, M.P.: PM_{2.5} : global progress in controlling the motor vehicle contribution. *Front. Environ. Sci. En.*, 8(1),
29 1-17, 2014.
- 30 Wang, H., Fu, L., Lin, X., Zhou, Y., Chen, J.: A bottom-up methodology to estimate vehicle emissions for the
31 Beijing urban area. *Sci. Total Environ.*, 407(6), 1947-1953, 2009
- 32 Wang, X., Westerdahl, D., Wu, Y., Pan, X., Zhang, K.M.: On-road emission factor distributions of individual
33 diesel vehicles in and around Beijing, China. *Atmos. Environ.*, 45(2), 503-513, 2011.
- 34 Wang, X., Westerdahl, D., Hu, J., Wu, Y., Yin, H., Pan, X., Zhang, K. M.: On-road diesel vehicle emission
35 factors for nitrogen oxides and black carbon in two Chinese cities. *Atmos. Environ.*, 46, 45-55, 2012a.
- 36 Wang, Z., Wu, Y., Zhou, Y., Li, Z., Wang, Y., Zhang, S., Hao, J.: Real-world emissions of gasoline passenger
37 cars in Macao and their correlation with driving conditions. *Int. J. Environ. Sci. Techno.*, 11(4),
38 1135-1146, 2014
- 39 Wang, R., Wu, Y., Ke, W., Zhang, S., Zhou, B., Hao, J.: Can propulsion and fuel diversity for the bus fleet
40 achieve the win-win strategy of energy conservation and environmental protection? *Appl. Energy*, 147,
41 92-103, 2015.



- 1 Wu, Y., Wang, R., Zhou, Y., Lin, B., Fu, L., He, K., Hao, J.: On-Road vehicle emission control in Beijing: past,
2 present, and future. *Environ. Sci. Technol.*, 45(1), 147–153, 2011.
- 3 Wu, X., Zhang, S., Wu, Y., Un, P., Ke, W., Fu, L., Hao, J.: On-road measurement of gaseous emissions and fuel
4 consumption for two hybrid electric vehicles in Macao. *Atmos. Pollu. Res.*, 6, 858-866, 2015.
- 5 Wu, X., Zhang, S., Wu, Y., Li, Z., Fu, L., Hao, J.: Real-World Emissions and Fuel Consumption of Diesel Buses
6 and Trucks in Macao: From On-road Measurement to Policy Implications. *Atmos. Environ.*, 120, 393-403,
7 2015.
- 8 Zannetti, P.: *Air Pollution Modeling*. Springer US, 1990.
- 9 Zhang, S., Wu, Y., Liu, H., Wu, X., Zhou, Y., Yao, Z., Fu, L., He, K., Hao, J.: Historical evaluation of vehicle
10 emission control in Guangzhou Based on a multi-year emission inventory. *Atmos. Environ.*, 76, 32-42,
11 2013.
- 12 Zhang, S., Wu, Y., Wu, X., Li, M., Ge, Y., Liang, B., Xu, Y., Zhou, Y., Liu, H., Fu, L., Hao, J.: Historic and
13 future trends of vehicle emissions in Beijing, 1998–2020: A policy assessment for the most stringent
14 vehicle emission control program in China. *Atmos. Environ.*, 89, 216-219, 2014a.
- 15 Zhang, S., Wu, Y., Liu, H., Huang, R., Un, P., Zhou, Y., Fu, L., Hao, J.: Real-world fuel consumption and CO₂
16 (carbon dioxide) emissions by driving conditions for light-duty passenger vehicles in China. *Energy*, 69,
17 247-257, 2014b.
- 18 Zhang, S., Wu, Y., Liu, H., Huang, R., Yang, L., Li, Z., Fu, L., Hao, J.: Real-world fuel consumption and CO₂
19 emissions of urban public buses in Beijing. *Applied Energy*, 113, 1645-1655, 2014c
- 20 Zhang, S., Wu, Y., Hu, J., Huang, R., Zhou, Y., Bao, X., Fu, L., Hao, J.: Can Euro V heavy-duty diesel engines,
21 diesel hybrid and alternative fuel technologies mitigate NO_x emissions? New evidence from on-road tests
22 of buses in China. *Appl. Energy*, 132, 118-126, 2014d
- 23 Zheng, B., Huo, H., Zhang, Q., Yao, Z.L., Wang, X.T., Yang, X.F., Liu, H., He, K.B.: High-resolution mapping
24 of vehicle emissions in China in 2008. *Atmos. Chem. Phys.*, 14, 9787-9805, 2014
- 25 Zheng, X., Wu, Y., Jiang, J., Zhang, S., Liu, H., Song, S., Li, Z., Fan, X., Fu, L., Hao, J.: Characteristics of
26 on-road diesel vehicles: Black carbon emissions in Chinese cities based on portable emissions
27 measurement. *Environ. Sci. Technol.*, accepted, 2015
- 28 Zhou, Y., Wu, Y., Yang, L., Fu, L., He, K., Wang, S., Hao, J., Chen, J., Li, C.: The impact of transportation
29 control measures on emission reductions during the 2008 Olympic Games in Beijing, China. *Atmos.*
30 *Environ.*, 44, 285-293, 2010.
- 31 Zhou, Y., Wu, Y., Zhang, S., Fu, L., Hao, J.: Evaluating the emission status of light-duty gasoline vehicles and
32 motorcycles in Macao with real-world remote sensing measurement. *J. Environ. Sci.*, 26(11): 2240-2248,
33 2014.

34



1 Tables

2

 3 **Table 1.** 24-h allocations of total traffic counts by region and road class during weekdays in Macao,
 4 2010

Region		The Macao Peninsula			The Taipa-CoTai-Coloane Region		
Road classes	Freeway	Arterial	Residential	Freeway	Arterial	Residential	
0	0.021	0.017	0.021	0.021	0.017	0.022	
1	0.013	0.014	0.013	0.013	0.014	0.013	
2	0.011	0.009	0.011	0.011	0.010	0.011	
3	0.009	0.007	0.009	0.009	0.007	0.009	
4	0.008	0.007	0.008	0.008	0.007	0.008	
5	0.008	0.008	0.008	0.008	0.008	0.008	
6	0.021	0.024	0.020	0.021	0.024	0.021	
7	0.029	0.051	0.029	0.029	0.022	0.030	
8	0.051	0.057	0.059	0.048	0.053	0.061	
9	0.048	0.054	0.048	0.042	0.052	0.051	
10	0.044	0.049	0.050	0.046	0.055	0.049	
11	0.055	0.050	0.049	0.056	0.056	0.048	
12	0.051	0.056	0.055	0.051	0.056	0.058	
13	0.059	0.062	0.061	0.062	0.064	0.062	
14	0.060	0.066	0.064	0.070	0.073	0.059	
15	0.064	0.061	0.059	0.068	0.072	0.065	
16	0.066	0.061	0.060	0.071	0.070	0.046	
17	0.066	0.066	0.059	0.065	0.069	0.069	
18	0.071	0.066	0.076	0.062	0.060	0.070	
19	0.061	0.057	0.062	0.054	0.051	0.075	
20	0.049	0.045	0.052	0.049	0.046	0.045	
21	0.048	0.041	0.052	0.048	0.042	0.050	
22	0.047	0.039	0.042	0.047	0.039	0.039	
23	0.042	0.033	0.032	0.042	0.034	0.033	

5



1 **Table 2.** Summary of age allocation for on-road fleets by vehicle classification in Macao

Vehicle classification	LDPV		MC		Taxi	PB		MDPV		HDPV	LDT		HDT	
Sub-classification	G ^a	D ^b	Heavy ^c	Light ^c	D	Medium ^d	Heavy ^d	G	D	D	G	D	D	
Ratio	0.99	0.01	0.68	0.32	1.00	0.33	0.67	0.53	0.47	1.00	0.25	0.75	1.00	
Vehicle age	1	0.12	0.12	0.18	0.09	0.14	0.00	0.08	0.20	0.16	0.20	0.12	0.08	0.02
	2	0.10	0.17	0.15	0.08	0.13	0.00	0.08	0.17	0.17	0.06	0.17	0.18	0.15
	3	0.10	0.08	0.19	0.09	0.04	0.00	0.08	0.07	0.12	0.09	0.11	0.10	0.11
	4	0.10	0.11	0.14	0.07	0.06	0.00	0.18	0.06	0.02	0.10	0.03	0.09	0.04
	5	0.09	0.03	0.08	0.04	0.06	0.17	0.16	0.05	0.09	0.09	0.03	0.05	0.03
	6	0.06	0.05	0.05	0.07	0.02	0.12	0.14	0.05	0.03	0.09	0.09	0.04	0.01
	7	0.05	0.01	0.04	0.04	0.11	0.25	0.15	0.06	0.01	0.03	0.00	0.02	0.01
	8	0.05	0.02	0.04	0.07	0.16	0.05	0.05	0.08	0.01	0.05	0.05	0.02	0.00
	9	0.04	0.03	0.02	0.08	0.24	0.00	0.00	0.04	0.01	0.05	0.02	0.02	0.01
	10	0.04	0.06	0.01	0.13	0.01	0.07	0.00	0.06	0.02	0.04	0.01	0.03	0.02
	11	0.05	0.06	0.03	0.14	0.03	0.17	0.01	0.02	0.01	0.10	0.02	0.04	0.01
	12	0.05	0.04	0.02	0.06	0.00	0.00	0.03	0.03	0.01	0.04	0.01	0.04	0.02
	13	0.03	0.06	0.00	0.01	0.00	0.03	0.00	0.02	0.03	0.00	0.02	0.02	0.01
	14	0.04	0.05	0.01	0.01	0.00	0.10	0.00	0.02	0.03	0.00	0.06	0.04	0.04
	15	0.03	0.05	0.01	0.01	0.00	0.05	0.00	0.04	0.05	0.00	0.06	0.04	0.11
	16	0.02	0.02	0.01	0.00	0.00	0.00	0.00	0.03	0.04	0.03	0.04	0.06	0.16
	17	0.01	0.03	0.00	0.01	0.00	0.00	0.00	0.00	0.03	0.00	0.05	0.04	0.06
	18	0.01	0.01	0.00	0.00	0.00	0.00	0.00	0.00	0.06	0.00	0.05	0.03	0.03
	19	0.00	0.00	0.00	0.00	0.00	0.00	0.04	0.00	0.02	0.00	0.02	0.02	0.07
	20	0.00	0.01	0.00	0.00	0.00	0.00	0.00	0.00	0.07	0.02	0.03	0.05	0.08
Fleet-average vehicle age	6.7	7.3	4.4	7.2	5.8	8.6	5.5	5.7	7.9	6.0	8.1	8.1	11.4	

2 Note: ^a gasoline; ^b diesel; ^c breaking point of engine displacement 50 ml; ^d breaking point of engine displacement at 5.0 L.



1 **Table 3.** Spatially-explicit estimation of traffic counts in Macao

Region	Daily traffic counts by road class (10^5 veh)			Hour-based density of traffic volume (10^4 veh h ⁻¹ km ⁻²)	
	Freeway	Arterial	Residential	Daily average	Evening rush hour (6 p.m.)
Macao Peninsula	15.2	70.8	138.4	10.0	17.3
Saint Antony Parish	2.8	20.5	35.0	25.3	44.3
Taipa-Cotai-Coloane	6.9	13.9	28.8	1.0	1.5
Taipa	2.2	12.5	17.8	2.0	3.1
Cotai	3.6	1.4	7.1	0.8	1.3
Coloane	1.1		3.9	0.3	0.5
Total	22.2	84.7	170.2	3.8	6.5

2

3 **Table 4.** Estimated fleet-average emission factors under real-world driving conditions

Vehicle classification	Fleet-average emission factors (g km ⁻¹)				
	CO	THC	NO _x	PM _{2.5}	CO ₂
LDPV-Gasoline	1.74	0.34	0.28	0.006	263
MDPV-Gasoline	14.3	1.80	1.18	0.030	379
MDPV-Diesel	1.60	0.27	1.44	0.26	307
HDPV-Diesel	4.76	0.25	10.9	0.48	914
LDT-Gasoline	8.38	2.30	1.31	0.014	250
LDT-Diesel	1.69	0.65	4.03	0.35	485
HDT-Diesel	7.40	0.94	12.3	0.95	1010
Taxi	0.47	0.06	0.86	0.11	192
MC-Light	7.95	4.07	0.26	0.030	39
MC-Heavy	10.2	1.18	0.38	0.012	86
PB-Medium	2.45	1.09	6.50	0.32	555
PB-Heavy	6.05	0.35	15.8	0.57	1215

4

5



1 **Table 5.** Length-specific emission intensity of total vehicular emissions during a typical
 2 weekday of 2010

Region	Road class	Length-specific emission intensity (kg km ⁻¹ d ⁻¹)				
		CO	THC	NO _x	PM _{2.5}	CO ₂
Macao Peninsula	Freeway	147	28	43	2.6	9046
	Arterial	196	42	39	1.9	7819
	Residential	80	17	18	0.9	3741
Taipa-Cotai-Coloane	Freeway	78	13	43	2.9	7412
	Arterial	58	10	36	2.3	5948
	Residential	25	5	6	0.4	1909
Cross-sea bridges	Freeways	130	24	61	4.0	10813
Total	Freeway	117	22	49	3.1	9069
	Arterial	124	25	38	2.1	6846
	Residential	60	13	14	0.7	3081

3
 4 **Table 6.** Area-specific emission intensity of total vehicular emissions during a typical
 5 weekday of 2010

Region / Parish	Area-specific emission intensity (kg km ⁻² d ⁻¹)				
	CO	THC	NO _x	PM _{2.5}	CO ₂
Macao Peninsula	1387	297	312	15.5	63695
St. Lazarus Parish	3152	682	696	33.7	139276
St. Lawrence Parish	1421	303	305	15.4	61268
Our Lady Fatima Parish	1258	271	274	13.7	57362
St. Anthony Parish	2520	547	557	26.4	117967
Cathedral Parish	799	166	199	10.4	38585
Taipa	301	53	151	9.50	27977
CoTai Reclamation Area	163	28	71	4.67	14055
Coloane	51	11	15	0.88	4440
Total land area of Macao	590	121	169	9.42	33645

6
 7



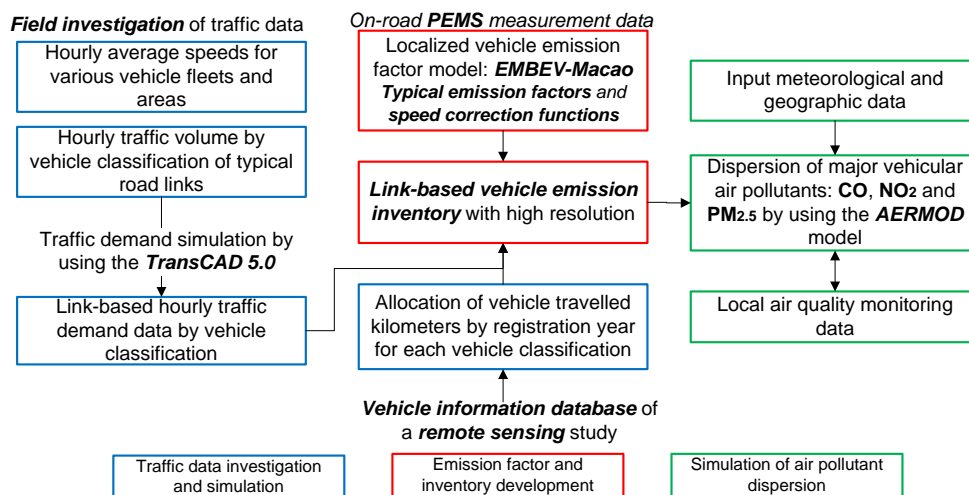
1 **Table 7.** Simulated average contributions contributed by primarily vehicular emissions in Macao, weekdays during November 2010

Region / Parish	Simulated concentrations of primary vehicular emissions ($\mu\text{g m}^{-3}$)								
	CO			NO ₂			PM _{2.5}		
	Mean	Min	Max	Mean	Min	Max	Mean	Min	Max
Macao Peninsula	205	59.5	424	42.3	14.3	84.9	2.03	0.67	3.89
St. Lazarus Parish	340	277	424	68.4	57.1	84.9	3.14	2.59	3.89
St. Lawrence Parish	186	143	272	37.1	27.9	52.6	1.72	1.32	2.47
Our Lady Fatima Parish	176	79.9	317	35.4	15.2	58.5	1.64	0.67	3.21
St. Anthony Parish	305	2306	372	60.5	44.7	74.5	2.85	2.17	3.39
Cathedral Parish	171	59.5	380	34.1	14.3	78.7	2.03	1.00	3.14
Taipa	44.1	13.2	109	16.7	4.32	40.9	1.65	0.61	2.46
CoTai Reclamation Area	38.9	11.7	66.1	14.8	4.10	27.6	1.08	0.27	2.39
Coloane	17.7	7.34	56.6	5.72	2.06	17.6	0.29	0.12	0.63
Total land area of Macao	87.7	7.34	424	22.2	2.06	84.9	1.30	0.12	3.89

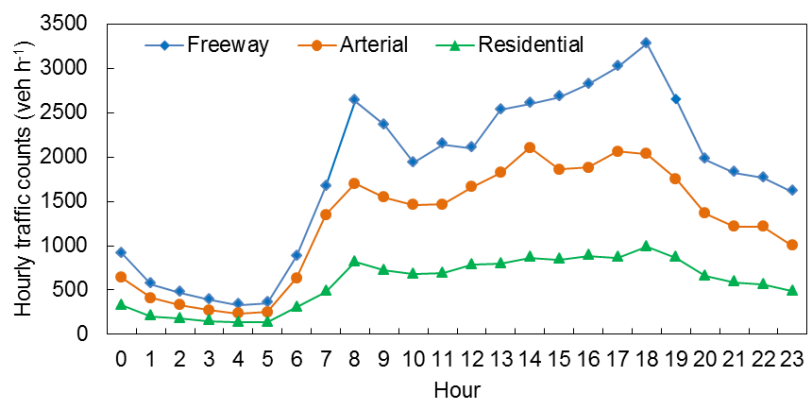
2 Note: Simulated results for November 6-8 are not accounted in this table due to the impact of rainfall. Mean, minimum and maximum
 3 values are for simulated average concentrations of each receptors in each region/parish during the study period.



1 **Figures**
2



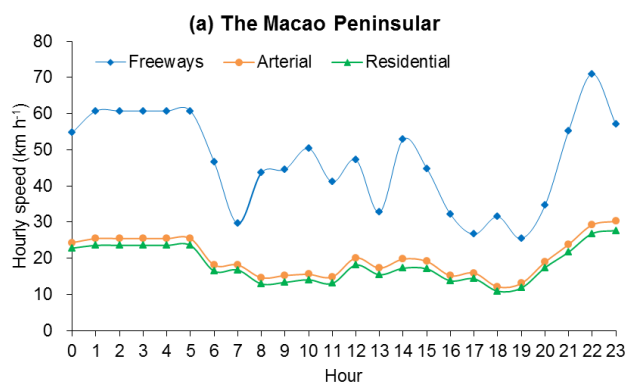
3
4 Fig. 1. Framework of high-resolution simulation for vehicle emissions and concentrations
5 of vehicular pollutants.
6



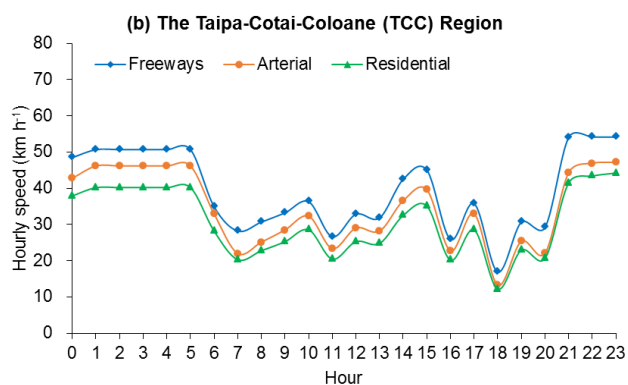
1
2 Fig. 2. Average hourly traffic accounts of observed links by road class during weekdays,
3 2010.
4
5



1



2



3

4

5 Fig. 3. Variations in aggregated hourly speeds by road class and region for LDPVs during
6 weekdays, 2010.

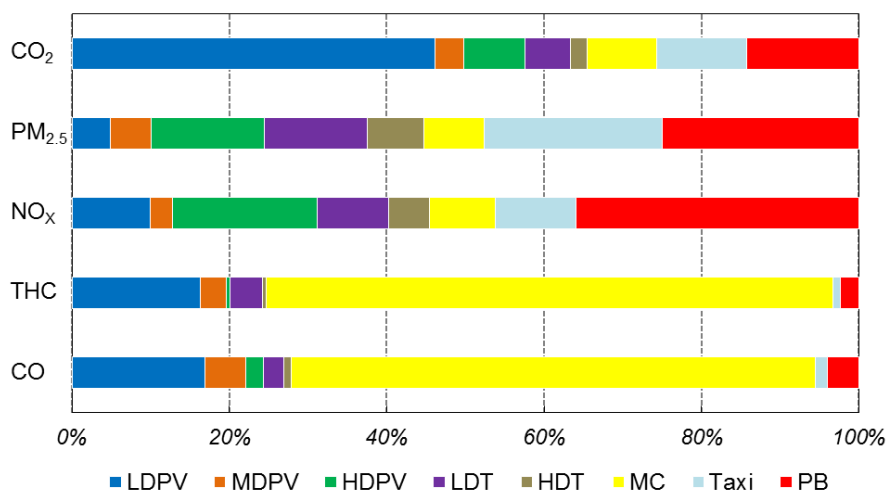
7

8

9



1



2

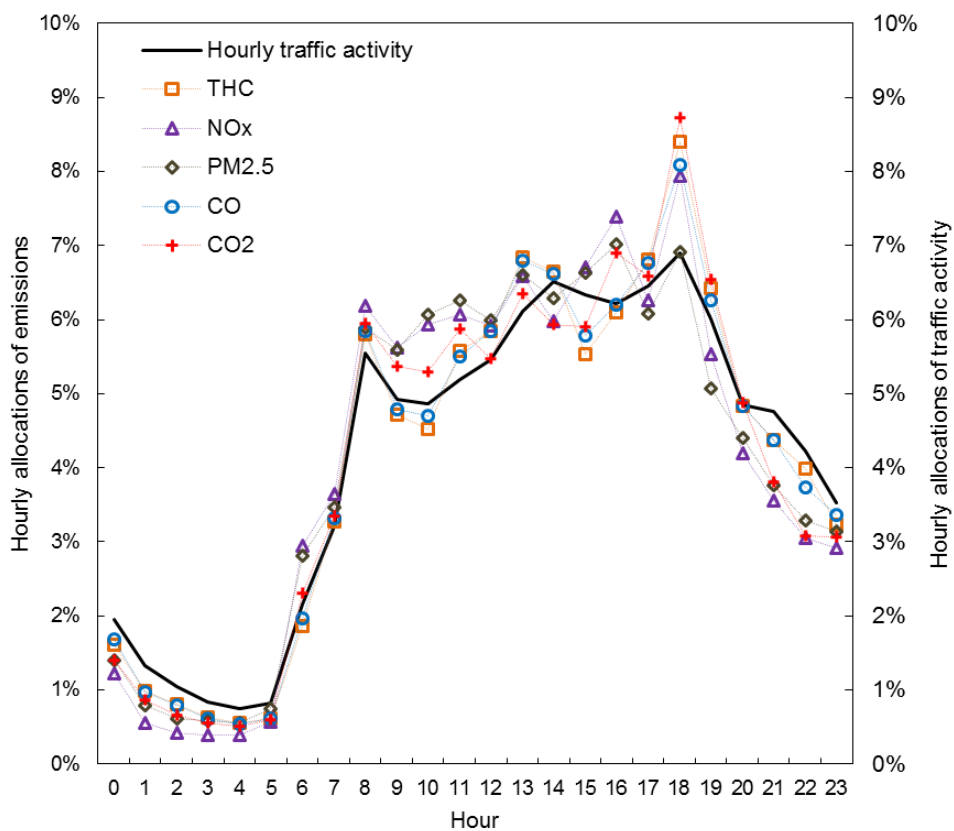
3

4

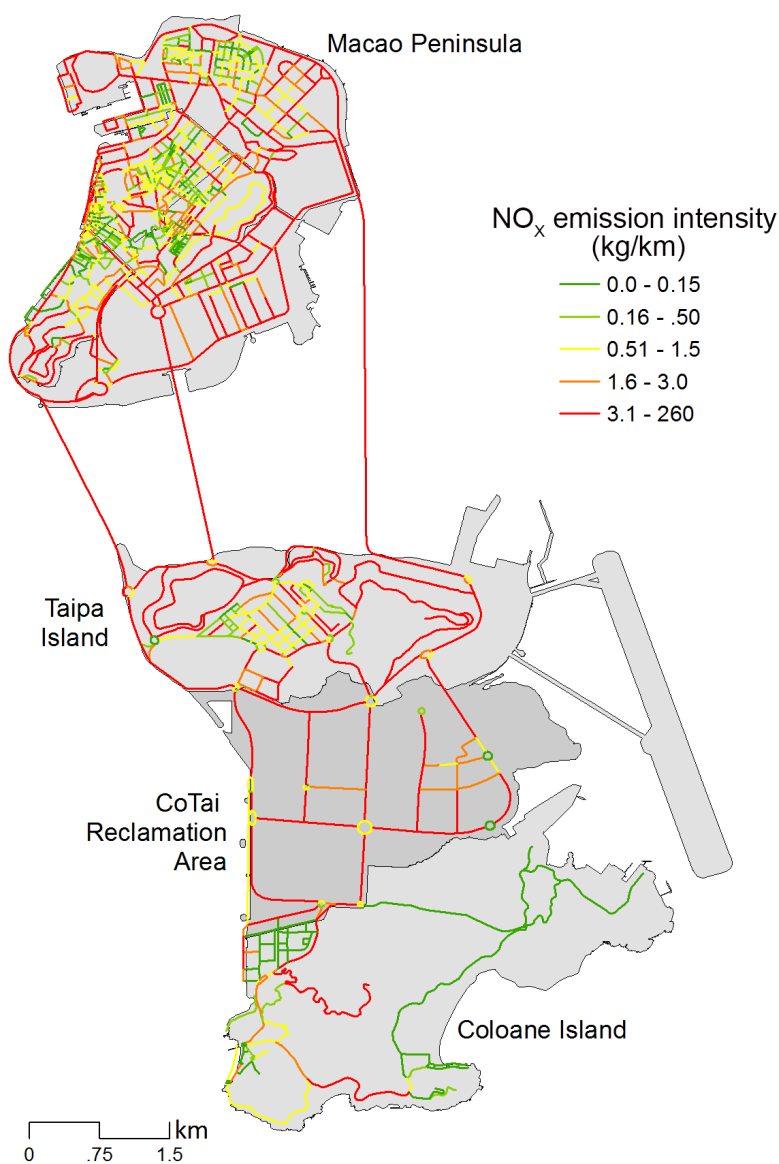
Fig. 4. Allocations of total vehicular emissions by vehicle classification

5

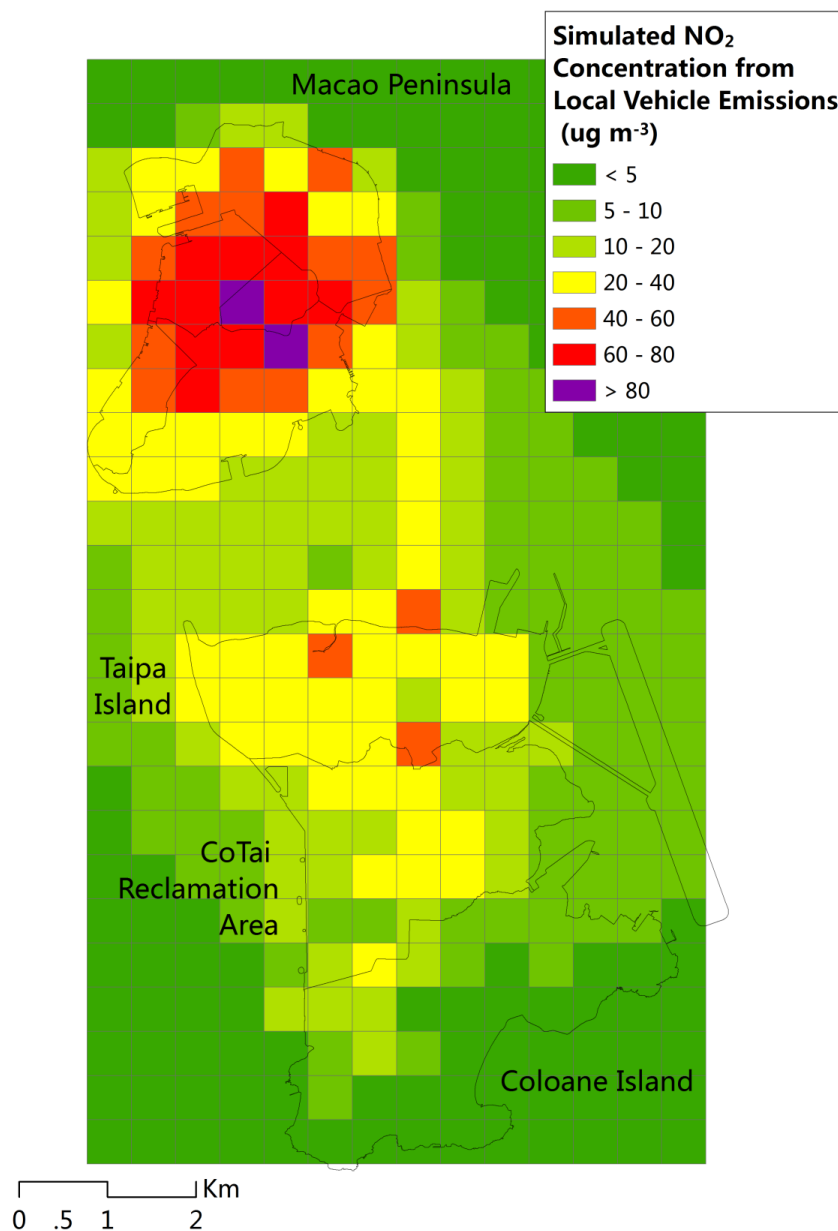
6



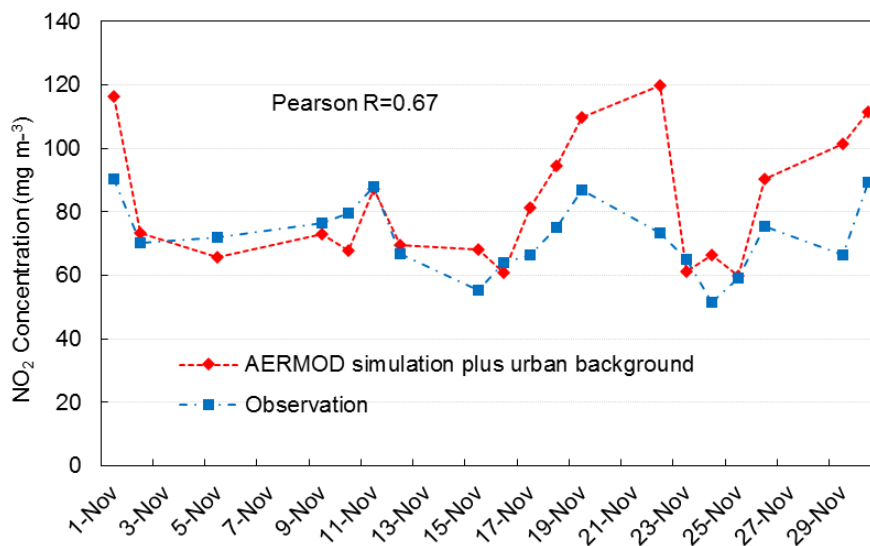
1
2 Fig. 5. Hourly allocations of vehicular emissions and traffic activity in Macao during
3 weekdays, 2010.
4



1
2 Fig. 6. The spatial distribution of NO_x emission intensity for on-road vehicles in Macao
3 during a typical weekday of 2010
4



1
2 Fig. 7. Simulated vehicle-contributed concentration of NO₂ in Macao during weekdays of
3 November, 2010
4
5



1
2 Fig. 8. Comparison of AERMOD simulated and observed daily NO₂ concentrations for
3 the traffic-populated site, 19 weekdays during November, 2010
4 Note: Simulated NO₂ concentrations during November 6-8 are significantly higher than
5 observed data probably due to the effect of rainfall, which are not included in this study.
6